Loop Closure and Trajectory Estimation with Long-Range Passive RFID in Densely Tagged Environments

Philipp Vorst, Bin Yang, and Andreas Zell

Abstract— **In more and more commercial scenarios, radio frequency identification (RFID) is used to tag assets on a large scale. These given tag infrastructures offer themselves for the navigation of autonomous transport vehicles and service robots. In this paper we investigate loop closure for graph-based simultaneous localization and mapping (SLAM) and trajectory estimation in environments with such dense RFID infrastructures: We compare different methods of inferring that a place has been revisited, examine their robustness, and show how the trajectory of the robot can be reconstructed. Given this trajectory, a robot is able to map transponder positions or to localize itself with RFID and odometry alone and without a reference localization system. The accuracy of our approach is shown through a series of experiments with a mobile robot.**

I. INTRODUCTION

In the near future, radio frequency identification (RFID) will be used for labeling products and assets in many commercial applications. Then, in supermarkets, warehouses, logistics centers, and production plants, RFID transponders will be deployed in considerable densities. Such transponders have unique identifiers and can be read by an RFID reader via electromagnetic waves. In the depicted applications, mobile robots can be employed for continuous inventory, transportation of goods, or customer assistance, for instance. By means of RFID readers and odometry for self-localization, enhanced by ultrasonic sensors for collision avoidance, robots will be able to navigate autonomously with low-cost sensors only.

In order to localize itself, a robot should be able to map its environment beforehand. In this paper, we show how the trajectory of the robot can be estimated without a prior map, using recent graph-based approaches to the simultaneous localization and mapping (SLAM) problem. Given the reconstructed trajectory, the robot is able to both map the positions of RFID tags (i.e., also the positions of tagged goods) [1], [2] and to keep a database of location fingerprints which can be used for RFID-based self-localization [3]. Our method is based on different models for loop closure with long-range passive RFID, which we compare. These models can be utilized in an arbitrary graph-based SLAM framework which represents observations as rigid body transformations with uncertainty estimates. Note that long-range RFID features read ranges of up to 10 m (short-range RFID: 1 m) and lacks distance information, contrary to active (battery-powered) RFID. Thus, although data association is trivial due to the unique identifiers of RFID tags, loop closure is not straightforward because of the large position uncertainty.

This work was funded by the Landesstiftung Baden-Württemberg in the scope of the research program BW-FIT, research cooperation AmbiSense.

P. Vorst and B. Yang are with the Chair of Computer Architecture, headed by Prof. A. Zell, Computer Science Department, University of Tübingen, Sand 1, D-72076 Tübingen, Germany {philipp.vorst, andreas.zell}@uni-tuebingen.de

This paper is organized as follows. In the next section, we describe related approaches. Then, in Sect. III, we briefly review graph-based SLAM and loop closure in general. In Sect. IV, we present how long-range RFID can be used for closing loops. Our models are experimentally investigated in Sect. V, and in Sect. VI we finally draw conclusions.

II. RELATED WORK

Loop closure with cameras or laser range finders is a well-studied topic. Because there are numerous publications, our subsequent survey only lists exemplary contributions. By means of 2-D and 3-D laser range finders, loops are closed by matching the latest scan with single scans [4] or a series of scans which have been assembled to a prior map estimate [5], [6]. Our approach is related insofar as we also perform a matching of measurements. This is similar to scan matching in some sense, although geometric information is missing almost entirely. In hybrid metric-topological approaches such as Atlas [7], local maps are matched against each other on a higher level to close large loops. Clemente *et al.* [8] mapped larger-scale outdoor scenes with a monocular camera. The geometric compatibility of correlating features in local maps indicated closed loops in their approach. Rybski *et al.* investigated graph-based SLAM in a setup with limited visual sensing capabilities [9]. It is similar to our approach, but the uncertainty of constraints was estimated from the number of competitive measurements which voted for a closed loop.

While all aforementioned methods explicitly perform loop-closure detection, it may be worth mentioning that in other approaches cycles are detected only implicitly. In particle filter-based SLAM, inconsistent maps are ruled out over time [10]. (Extended) Kalman filters, as also often used for SLAM, propagate back the uncertainty revealed by a closed loop over correlated landmark position estimates [11].

Regarding RFID-based works, Kleiner *et al.* performed graph-based SLAM and inferred a sparse network of short-range transponder positions [12]. Our approach differs in that we assume an environment with a high density of long-range RFID tags. Tanaka's approach [13] is between the one by Kleiner *et al.* and ours: It is based on stochastic gradient descent for inferring a network of transponder positions from short series of measurements, but his RFID tags are active and only sparsely distributed. Djugash *et al.* also researched into (range-only) SLAM with active RFID tags [14], but employed an extended Kalman filter.

III. BRIEF REVIEW OF GRAPH-BASED SLAM AND LOOP CLOSURE

Among the main paradigms of solving the problem of simultaneous localization and mapping (SLAM), graph-based SLAM makes use of nonlinear sparse optimization. The environment is considered to consist of a number of landmarks whose positions, along with past locations of the robot, are to be estimated. In order to do so, a graph is built whose nodes represent the landmark and robot locations, and edges are given by geometric constraints between the nodes. There are two types of constraints: measured displacements between consecutive robot poses (odometry), and observed displacements between nodes. The latter type of constraints may consist of coordinates of observed features in the environment, relative to a robot location, or displacements between not directly consecutive robot locations, which are estimated from observations. Since odometry and sensor readings are error-prone, each constraint is associated an error estimate. Solving graph-based SLAM consequently turns into finding a configuration of node locations which minimizes the overall error of the network. Its original solution dates back to Lu and Milios [4], but far more efficient approaches have been presented recently [15], [16], [17], the latter two based on stochastic gradient descent. Typically, the entire graph is batch-processed in an offline fashion, involving a series of nonlinear optimization steps.

Formally, let $\mathbf{X}_{0:T} = (\mathbf{x}_0, \ldots, \mathbf{x}_T)$ denote the path of the robot (to be estimated) up to time step T, with $\mathbf{x}_t = (x_t, y_t, \theta_t)$ the global 2-D coordinates and heading of the robot at time t. Let $\mathbf{Z}_{0:T} = (\mathbf{z}_1, \ldots, \mathbf{z}_T)$ be the sequence of observations and $\mathbf{U}_{0:T} = (\mathbf{u}_1, \ldots, \mathbf{u}_T)$ be the series of movements. And let $\mathbf{m}$ be the map, i.e., a vector of landmark locations to be estimated. Then, computing the SLAM solution equals [18] maximizing the log-posterior

$$\begin{aligned} &\log p(\mathbf{X}_{0:T}, \mathbf{m} \,|\, \mathbf{Z}_{0:T}, \mathbf{U}_{0:T}) \qquad (1) \\ &= \sum_t \log p(\mathbf{x}_t \,|\, \mathbf{x}_{t-1}, \mathbf{u}_t) + \sum_t \log p(\mathbf{z}_t \,|\, \mathbf{x}_t, \mathbf{m}) + const, \end{aligned}$$

where $p(\mathbf{x}_t \,|\, \mathbf{x}_{t-1}, \mathbf{u}_t)$ represents the motion model and $p(\mathbf{z}_t \,|\, \mathbf{x}_t, \mathbf{m})$ the sensor model. A uniform treatment of constraints is possible if $\mathbf{X}$ is the overall configuration of node locations (robot poses, optionally plus landmark locations) and constraints are regarded as rigid-body transformations with expected values δ and associated error covariance matrices Σ, as in [16], [17]. Then, maximizing (1) turns into minimizing

$$-\log p(\mathbf{X}) \propto (f(\mathbf{X}) - \delta))^T \Sigma^{-1} (f(\mathbf{X}) - \delta)) \qquad (2)$$

where $f(\mathbf{X})$ generates zero-noise observations according to the current configuration $\mathbf{X}$. It often suffices to recover only the trajectory of the robot, $\mathbf{X}_{0:T}$, since given the trajectory, a map of the environment can be built in a second offline batch-processing step.

One key feature of SLAM algorithms is the closing of loops, that is, the ability to treat the situation that the robot has revisited the same place. This must be possible even if the uncertainty in the pose of the robot is large. Loop closure is important because it enables the robot to correct odometric errors that were accumulated along its path. In graph-based SLAM, loop closure is done by adding a constraint which relates two (nonconsecutive) poses of the robot. Thus, first it requires the identification of two similar or equal positions by means of sensor measurements. Second, a metric transformation between the positions with corresponding error estimate must be provided. With RFID sensors, the former part is trivial, since tag IDs are unique and indicate that the robot has re-entered the read range of some transponder. The second step, however, is not that easy, because – due to a read range of up to 10 m – the position uncertainty of RFID measurements can be even larger than accumulated odometric errors.

IV. LOOP CLOSURE WITH RFID

A. RFID Fingerprints

In our approach, we utilize the fact that radio frequency identification (RFID) allows for the unique identification of small transponders (also called tags) via radio waves. That is, an on-board RFID reader frequently emits electromagnetic waves, which power nearby RFID tags and enable them to send back their IDs. Passive UHF (∼900 MHz band) RFID tags, as used in our study and also for commercial labeling of pallets and products, have a read range of several meters. The chance of detecting an RFID tag largely depends on its distance and relative angle to the antenna of the RFID reader. Tag detections are further dependant on a number of physical phenomena such as reflection and absorption by nearby objects (especially those made of metal or containing water) and multi-path effects. It is almost impossible to model such factors, because it would require detailed knowledge of the structure and composition of the environment. Models of RFID detection rates would accept those factors as noise, which results in less accurate navigation performance. Quite the contrary, in our approach, we make use of all influencing factors, but do not model them explicitly: We regard local RFID measurements as fingerprints of their recording position. These fingerprints are highly location-specific [19] in terms of expressiveness, especially if the tag density is high [3]. RFID fingerprints are similar to appearance-based methods used for SLAM or self-localization, where features extracted from images characterize the position where the images were taken. Analogously, the detection of an RFID tag resembles the presence of a single image feature.

B. Establishing Loop Closures

With regard to Sect. III, we aim at performing loop closure by detecting that some place is revisited. So, a closed loop must be inferred from the comparison of the current RFID measurements to previously recorded fingerprints. Consequently, we would like to determine the degree of similarity of measurements, and if the similarity exceeds some threshold ϑ_S, we will add a loop-closure constraint to the SLAM graph. So, two issues have to be solved: How to compute similarities of RFID measurements, and how to

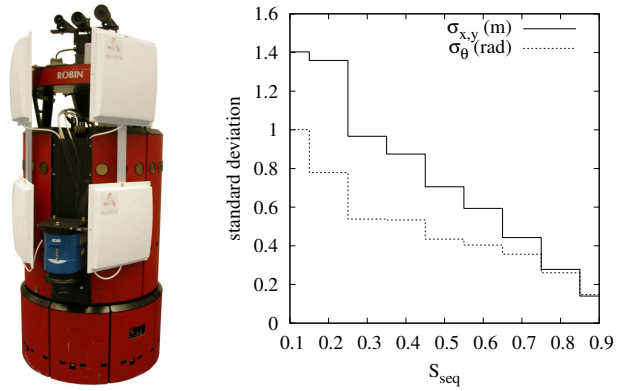

Fig. 1. Left: The mobile robot (B21) used for the experiments, with its UHF RFID antennas (white), spanning an angle of approx. 90°. Right: Standard deviations of distances and angles between the recording positions of two fingerprint sequences (sequence length was $\vartheta_D = 3.0\,m$), learned from training data. The plot shows the uncertainties depending on different similarity values S_{seq} with histogram resolution 0.1. As can be seen, for instance, two sequences of high similarity 0.9 can be expected to be recorded in very similar poses (distance 0.14 m, angular difference 0.15 rad).

parameterize the constraint. We will dedicate to the first issue in the next section, where we present measures of RFID fingerprint similarity. The second issue, the parameterization of the constraint, has to overcome one central problem of passive long-range RFID: RFID measurements neither disclose distances nor bearings to a tag. Hence, it is virtually impossible to estimate displacements between the recording positions of distinct measurements. This is an inherent difference to laser range finder-based navigation, for example, where scan matching yields transformations between the recording positions of two or several scans.

That is why we propose a different solution: We assume that we can detect sufficiently accurately if the robot revisits some position, based on the similarity measures presented below. If two RFID measurements at times t and t' match well, we will infer that their recording positions are identical. That is, we will add a constraint $\delta_{t,t'} = (0, \ldots, 0)$, with all components zero, to the graph. As an estimate of the corresponding uncertainty, $\Sigma_{t,t'}$, one can choose a diagonal matrix with small values on its main diagonal, expressing that the transformation is only induced if places are very similar. Our suggestion is to take a step ahead and calibrate the loop closure model in a training phase beforehand. This calibration is treated in Sect. IV-D, based on the similarity measures that we present in the next section.

C. Measures of RFID Fingerprint Similarity

We formally represent a fingerprint $\mathbf{F}_t$ at time t by a pair $\mathbf{F}_t = (\mathbf{f}_t, \mathbf{x}_t)$. $\mathbf{x}_t = (x_t, y_t, \theta_t)$ is the recording position and heading of the robot. (During trajectory estimation, this pose is unknown.) $\mathbf{f}_t = (\mathbf{f}_{t,l}, \mathbf{f}_{t,r})$, with $\mathbf{f}_{t,a} = (f_{t,a}^{(1)}, \ldots, f_{t,a}^{(K)})$ (antenna $a \in \{l, r\}$), is the result of an inquiry that was carried out for all antennas connected to the RFID reader. In our case, the robot possesses two pairs of antennas (Fig. 1), pointing to the left (l) and to the right (r). $f_{t,a}^{(k)}$ counts how often antenna pair a has detected tag k. K is the total number of tags that are observable in the environment.

In the following, we introduce three similarity measures for two fingerprints. As a requirement, similarity values should lie in $[0.0; 1.0]$, as usual. Moreover, we would like to exploit the directionality of RFID fingerprints that are taken with antennas pointing towards different directions.

1) Comparing pairs of single measurements: Let $\mathbf{f}_{t,a}$ and $\mathbf{f}_{t',a}$ denote two tag lists, taken at time t and t', respectively. Each tag list contains the observations for the same antenna a, but at different recording positions. In order to compare them, we employ the cosine similarity:

$$\cos(\mathbf{f}_{t,a}, \mathbf{f}_{t',a}) = \frac{\sum_{k=1}^{K} f_{t,a}^{(k)} f_{t',a}^{(k)}}{\sqrt{\sum_{k=1}^{K} \left(f_{t,a}^{(k)}\right)^2} \cdot \sqrt{\sum_{k=1}^{K} \left(f_{t',a}^{(k)}\right)^2}} \quad (3)$$

This gives a similarity in $[0.0; 1.0]$ for a single antenna, because detection counts are nonnegative. Visually, the computed value is the cosine of the angle spanned by the vectors $\mathbf{f}_t$ and $\mathbf{f}_{t'}$. The similarity S_{single} of two entire fingerprints at different recording positions can then be computed by

$$S_{single}(\mathbf{F}_t, \mathbf{F}_{t'}) = \prod_{a \in \{l,r\}} \cos(\mathbf{f}_{t,a}, \mathbf{f}_{t',a}) \quad (4)$$

That is, we multiply the pairwise similarities of the measurements of both sides, yielding a similarity value in $[0.0; 1.0]$.

2) Comparing pairs of sequences of measurements: A single RFID inquiry is prone to noise and can either detect or not detect a transponder. It is therefore reasonable to combine several measurements to a more robust, graded local estimate of detection rates. Prior experiments showed that mean detection rates are reproducible if the robot moves short distances only. Consequently, at each time step t, a new combined fingerprint is created by averaging over the most recent raw measurements while the robot is moving. Hence, the combined fingerprint $\overline{\mathbf{f}}_{t,a}$, $a \in \{l, r\}$, averages over n_t recent measurements $\mathbf{f}_{t-i,a}$, $i = 0, 1, \ldots$, for which $\sqrt{(x_t - x_{t-i})^2 + (y_t - y_{t-i})^2} \leq \vartheta_D$ holds for some distance threshold ϑ_D. The average detection rate of some tag k for antenna a then is:

$$\overline{f}_{t,a}^{(k)} = \frac{1}{n_t} \sum_{i=0}^{n_t - 1} f_{t-i,a}^{(k)} \quad (5)$$

For comparing the measurement sequences, we again employ the cosine similarity and obtain as the similarity S_{seq} of two entire combined fingerprints $\mathbf{F}_t$ and $\mathbf{F}_{t'}$:

$$S_{seq}(\mathbf{F}_t, \mathbf{F}_{t'}) = \prod_{a \in \{l,r\}} \cos(\overline{\mathbf{f}}_{t,a}, \overline{\mathbf{f}}_{t',a}) \quad (6)$$

3) Comparing pairs of measurement sequences with local adaptation: The previous technique of matching sequences of measurements is supposed to be more robust to noisy detection events. Yet, we can still improve robustness by distinguishing the importances of detected tags. Our goal is to identify locally dominant transponders and to achieve some further robustness to local variations in the number of observable tags: Even in densely tagged environments,

one does not expect perfect homogeneity with respect to tag density.

In order to achieve this, we adapt a technique that is known from the field of document retrieval: We compute a score for matching two RFID fingerprints, based on *term frequency*. First, we count the detection frequency of a tag k detected by antenna a among the closest, most recent n_t measurements:

$$d_{t,a}^{(k)} = \sum_{i=0}^{n_t-1} f_{t-i,a}^{(k)} \tag{7}$$

The weight of tag k is then defined by

$$w_{t,a}^{(k)} = \frac{d_{t,a}^{(k)}}{\sum_{j=1}^{K} d_{t,a}^{(j)}} \tag{8}$$

In analogy to document retrieval, this weight equals the term frequency of tag k among the tag detections in all recent fingerprints. It is important to note that these weights are also used for the measurement sequence to be compared with. This weighting achieves the adaptation to location-specific tag density. Now, the *score* of the measurement with antenna a for one recent fingerprint $\mathbf{f}_{t-i,a}$ is determined by

$$s_{t-i,a} = \sum_{k=1}^{K} f_{t-i,a}^{(k)} \, w_{t-i,a}^{(k)}, \quad i = 0, \ldots, n_t - 1 \tag{9}$$

Again, we multiply the scores of both antennas to obtain the score of the entire fingerprint:

$$s_{t-i} = \prod_{a \in \{l,r\}} s_{t-i,a} \tag{10}$$

Regarding the sequence of all previous n_t measurements, the average score $\overline{s}_t$ is

$$\overline{s}_t = \frac{1}{n_t} \sum_{i=0}^{n_t} s_{t-i} \tag{11}$$

The final step is to compute a similarity value $S_{term} \in [0.0; 1.0]$ from the scores of two measurement sequences:

$$S_{term}(\mathbf{F}_t, \mathbf{F}_{t'}) = \frac{\min(\overline{s}_t, \overline{s}_{t'})}{\max(\overline{s}_t, \overline{s}_{t'})} \tag{12}$$

For both S_{seq} and S_{term}, it is benefial to enforce a minimum number of fingerprints over which is averaged (e.g., three per meter). This increases robustness to noisy RFID data.

D. Model Calibration

All constraints in the SLAM graph require uncertainty estimates. For odometry-based edges, an estimate is derived from the robot's motion model. Its parameters are usually determined in prior experiments. Analogously, we can obtain a model of uncertainty for the employed similarity measure of RFID fingerprints. We therefor collect a number of fingerprints in a training phase and annotate them with their true positions. For each pair of measurements, we compute the degree of similarity and the displacement of their recording positions. Then, for small intervals of similarity values, the covariance of displacements can be computed. As an example, Fig. 1 illustrates the standard deviations obtained for different values of S_{seq}.

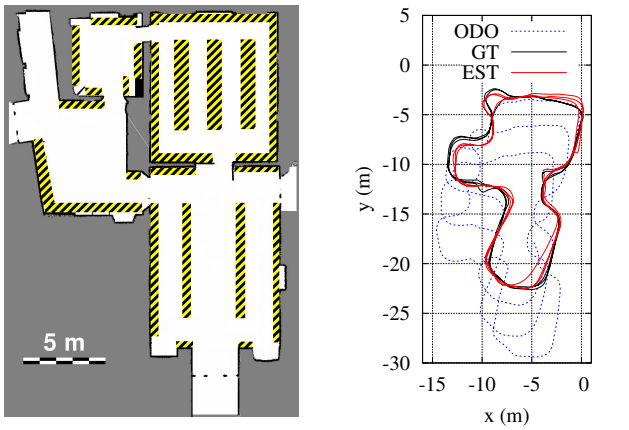

Fig. 2. Left: The environment in which we conducted our experiments. RFID tags were situated in the hatched areas. Right: An example of an estimated trajectory, obtained with measure S_{term}, $\vartheta_S = 0.7$, $\vartheta_D = 1.0$. ODO is the path given by pure odometry, GT is laser-based ground truth, and EST is the trajectory corrected with our method.

V. EXPERIMENTS

A. Setup

We conducted several experiments with a mobile robot in two different indoor environments. The mobile platform was an RWI B21 with a laser range finder (for ground truth only), an Alien Technology ALR-8780 UHF RFID reader (EPC Cl. 1 Gen. 2, 2 W EIRP transmitting power). Two pairs of RFID antennas are connected to the reader, which point at angles of approx. 45° to either side of the robot (Fig. 1, left). Their scan areas overlap only slightly, and RFID fingerprints feature a high level of directionality. The first experimental environment is shown in Fig. 2 (left). It has a size of approx. 195 m^2 and contains several loops and short corridors, similarly to a supermarket. Along those passages, we attached more than 400 tags in total at different heights and orientations. We recorded RFID data and odometry for ten different trajectories containing loops, each of which had a length of 68-295 m, corresponding to durations of 4-14 minutes and 313-1213 RFID measurements. These data were used for the experiments described below. The second environment was similar in size and shape, but it contained fewer tags. There, we recorded a dataset with six trajectories containing loops.

In the training phase, we collected RFID data and laser-based reference positions for the model calibration as described in Sect. IV-D. The training environment was a corridor (28 m×3 m) in which we spread 240 UHF RFID tags. We steered the robot manually on arbitrary paths along the corridor. On a trajectory length of 727 m corresponding to a duration of 41 minutes, 10613 fingerprints were taken. The recorded data were used to learn the constraint uncertainties.

B. Consistency of Estimated Trajectories

We measured the consistency of the trajectories that are obtained by closing loops with our approach. For optimizing the graph of constraints, we used the tree-based network optimizer TORO by Grisetti *et al.* [17]. As a measure of

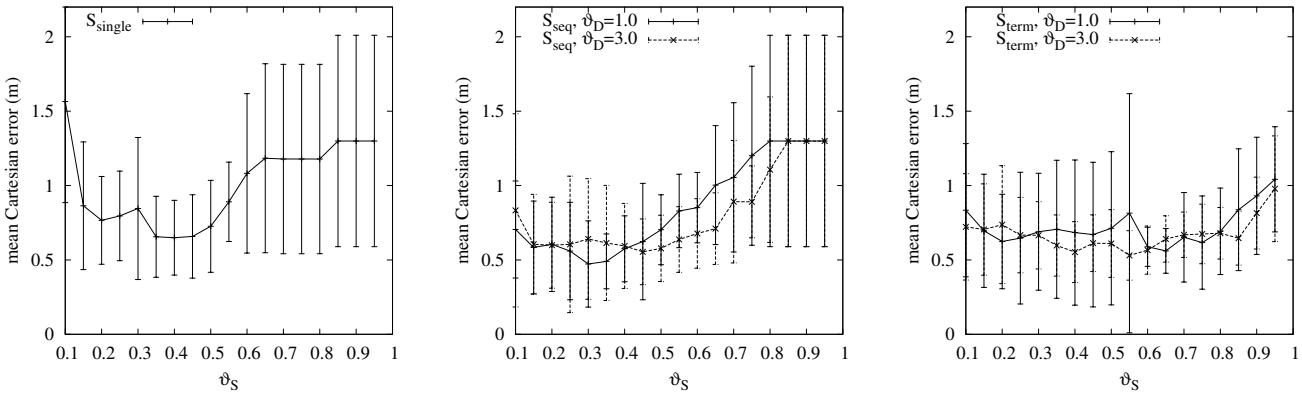

Fig. 3. Residual Cartesian errors and standard deviations, depending on the choice of the similarity threshold ϑ_S, for the different similarity measures and distances ϑ_D over which measurements are averaged. (The results for $\vartheta_D = 2.0$ are not shown for the sake of clarity, but are between the other ones.)

accuracy, we aligned the obtained trajectory at the ground truth trajectory and computed the mean Cartesian residual error on a per-node basis. Ground truth, with an average error of less than 0.1 m, was derived by laser-based Monte Carlo localization against a grid map learned beforehand. The residual Cartesian error of odometry alone was 1.23 m.

The results for the first dataset are shown in Fig. 3, in which we varied the combination distance threshold, ϑ_D (see IV-C.2), and the similarity threshold, ϑ_S (see IV-B). Further, we relaxed motion constraints by increasing their covariances. The Cartesian error for the best combinations of similarity measure and its parameters is approx. 0.47 m (S_{seq} with $\vartheta_S = 0.3$, $\vartheta_D = 1$). Similar values are achieved in a stable fashion over a large interval of ϑ_S, especially for S_{term}. This is important because in practice, the optimal choice of ϑ_S may vary for environments with different tag densities. Additionally, combining consecutive measurements improves the results w.r.t. to mean error and variance: The results of the similarity measure S_{seq} are better than the ones of S_{single}. Moreover, for the same measure, a larger distance ϑ_D appears to improve the stability of trajectory estimation w.r.t. to variance. This could be expected, because the larger ϑ_D, the more information is encoded in a combined measurement. Of course, the combination of long measurement sequences restricts the approach to environments with truly corridor-alike structures. A sample estimated trajectory in the first environment is visualized in Fig. 2 (right).

The second dataset achieved very similar results and has in common that variances are not always negligible (cf. Fig. 3). Some estimated trajectories were very accurate, with errors of approx. 0.2 m, others topologically satisfactory, but rather inaccurate, with errors of approx. 1.0 m. We found that inaccurately placed loop-closure constraints did occur sometimes. Outlier rejection mechanisms for loop closing (e.g., like in [8], [20]), on which we are working currently, will help to solve this issue of further improved robustness.

C. Accuracy and Number of Loop-Closure Constraints

In order to explain the above findings, we examined the consistency of inferred constraints. Clearly, there is a trade-off in the choice of the threshold ϑ_S, stating above which level of similarity a loop-closure constraint will be inferred. A large value of ϑ_S will choose constraints with a high probability of low uncertainty. Then, however, potentially few similar poses will be recognized, and the odometric error will only slightly be corrected. Figure 4 shows the mean numbers of loop-closure constraints obtained at different similarity thresholds. The term frequency-based similarity measure, S_{term}, yields the largest number of constraints for most choices of ϑ_S. Even for a high similarity threshold ϑ_S, closed loops are detected quite reliably, which results in a larger number of corrective edges in the SLAM graph.

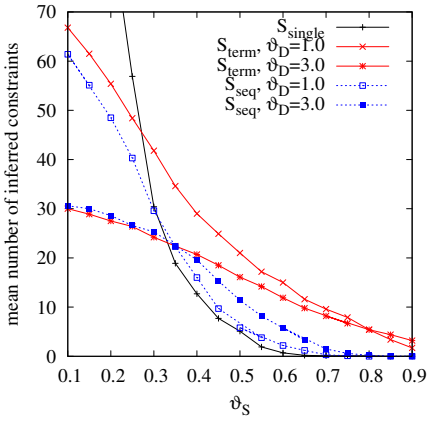

Fig. 4. Number of loop-closure constraints, depending on the choice of the similarity threshold ϑ_S, for the different similarity measures and distances ϑ_D over which measurements are averaged. (For the sake of clarity, values are cut at 70; the value of S_{single} for $\vartheta_S = 0.1$ was 223, decreasing monotonically thereafter.)

On the other hand, Fig. 5 shows the mean actual distances between nodes that are interconnected by loop-closure constraints. Since we are forced to add zero-edges when detecting a closed loop, these distances represent the error introduced right at loop-closure positions. Roughly, the most accurate trajectory estimates are achieved where small errors in the produced constraints meet fair numbers of inferred edges. S_{single} and S_{seq} yield the most accurate constraints, but at the expense that loop closures are detected at much lower rates. Beyond thresholds of 0.6 and 0.8, respectively, even no more constraints were found. Constraints indicated

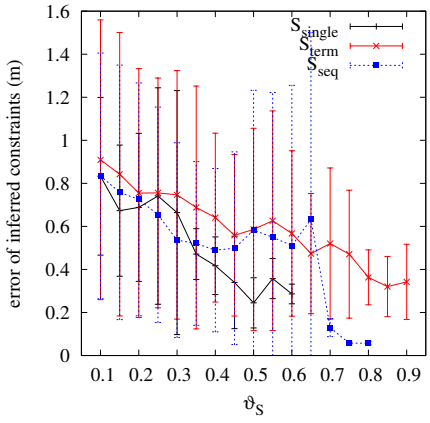

Fig. 5. Errors of loop-closure constraints in terms of actual distance between linked nodes, depending on the choice of the similarity threshold ϑ_S and for the three similarity measures. Here, we only focus on $\vartheta_D = 2.0$.

by S_{term} reveal slightly larger errors, but are detected more frequently even for larger similarity thresholds ϑ_S. A hybrid approach that selects the best similarity measure in a situation-dependant fashion suggests itself for future work.

VI. CONCLUSION

In this paper, we investigated loop closure with long-range passive RFID in environments with high tag densities. By detecting closed loops, a mobile robot was enabled to consistently estimate its trajectory. The contribution of this paper is the introduction and comparison of different loop closure models. We also showed how the underlying similarity measures can be integrated into a graph-based SLAM framework. An arising issue is the parameterization of the uncertainty of loop-closure constraints. Our solution to this is a calibration from training data. In a series of experiments, all presented models allowed for robust and quite accurate trajectory estimation on different datasets, where the term frequency-based measure revealed the best robustness to variations of the parameter ϑ_S. The best estimation error of approx. 0.5 m still differs from previous results in self-localization with RFID fingerprints [3]. There, however, the mean error of approx. 0.25 m was based on a prior map with a higher density of reference fingerprints.

The presented approach requires that places are revisited with similar orientations. This makes it suitable for environments with corridor structures (supermarkets and storehouses, for instance), which is not a substantial limitation: Such domains are those in which high tag densities can be expected in the near future. Although the chosen batch-processing paradigm is rather an offline approach, trajectory estimation can be performed in (or in close to) real-time because of the efficiency of the employed stochastic gradient descent framework [17]. In each cycle, loop closure detection lasted less than 10 ms on a 3 GHz CPU.

Usually, one will also be interested in landmark locations, i.e., the positions of RFID tags. The estimated trajectory can also be used to map the positions of RFID tags in order to, for instance, inventory and localize products. This is achieved by a second pass over the sensor data and the application of model-based mapping algorithms [1], [2]. Future work will also take the concurrent estimation of transponder positions into account, making our technique a full SLAM approach. Moreover, we are going to examine strategies to determine the best choice of the similarity threshold ϑ_S automatically.

REFERENCES

[1] D. Hähnel, W. Burgard, D. Fox, K. P. Fishkin, and M. Philipose, "Mapping and localization with RFID technology," in *Proc. 2004 IEEE Int. Conf. on Robotics and Automation (ICRA)*, 2004, pp. 1015–1020.

[2] T. Deyle, C. C. Kemp, and M. S. Reynolds, "Probabilistic UHF RFID tag pose estimation with multiple antennas and a multipath RF propagation model," in *Proc. 2008 IEEE/RSJ Int. Conf. on Intelligent Robots and Systems (IROS)*, Nice, France, 2008, pp. 1379–1384.

[3] P. Vorst, S. Schneegans, B. Yang, and A. Zell, "Self-localization with RFID snapshots in densely tagged environments," in *Proc. 2008 IEEE/RSJ Int. Conf. on Intelligent Robots and Systems (IROS)*, Nice, France, 2008, pp. 1353–1358.

[4] F. Lu and E. E. Milios, "Globally consistent range scan alignment for environment mapping," *Autonomous Robots*, vol. 4, no. 4, pp. 333–349, October 1997.

[5] J.-S. Gutmann and K. Konolige, "Incremental mapping of large cyclic environments," in *Proc. IEEE Int. Symposium on Computational Intelligence in Robotics and Automation (CIRA)*, 1999, pp. 318–325.

[6] A. Nüchter, K. Lingemann, J. Hertzberg, and H. Surmann, "6D SLAM – 3D mapping outdoor environments," *Journal of Field Robotics (JFR)*, vol. 24, no. 8-9, pp. 699–722, 2007.

[7] M. Bosse, P. Newman, J. Leonard, M. Soika, W. Feiten, and S. Teller, "An Atlas framework for scalable mapping," in *Proc. IEEE Int. Conf. on Robotics and Automation (ICRA '03)*, vol. 2, 2003, pp. 1899–1906.

[8] L. Clemente, A. Davison, I. Reid, J. Neira, and J. D. Tardós, "Mapping large loops with a single hand-held camera," in *Proc. Robotics: Science and Systems Conference*, 2007.

[9] P. E. Rybski, S. I. Roumeliotis, M. Gini, and N. Papanikolopoulos, "A comparison of maximum likelihood methods for appearance-based minimalistic SLAM," in *Proc. IEEE Int. Conf. on Robotics and Automation (ICRA)*, 2004, pp. 1777–1782.

[10] M. Montemerlo, S. Thrun, D. Koller, and B. Wegbreit, "FastSLAM: A factored solution to the simultaneous localization and mapping problem," in *Proc. AAAI National Conf. on Artificial Intelligence*. Menlo Park, CA, USA: AAAI, 2002, pp. 593–598.

[11] A. J. Davison, "Real-time simultaneous localisation and mapping with a single camera," in *Proc. IEEE Int. Conf. on Computer Vision (ICCV)*, vol. 2, 2003, pp. 1403–1410.

[12] A. Kleiner, C. Dornhege, and S. Dali, "Mapping disaster areas jointly: RFID-coordinated SLAM by humans and robots," in *Proc. IEEE Int. Workshop on Safety, Security and Rescue Robotics (SSRR)*, Rome, Italy, 2007.

[13] K. Tanaka, "Multiscan-based map optimizer for RFID map-building with low-accuracy measurements," in *Proc. 19th Int. Conf. on Pattern Recognition (ICPR)*, December 2008, pp. 1–4.

[14] J. Djugash, S. Singh, and P. I. Corke, "Further results with localization and mapping using range from radio," in *Int. Conf. on Field and Service Robotics (FSR)*, ser. Springer Tracts in Advanced Robotics, vol. 25. Springer Berlin/Heidelberg, 2005, pp. 231–242.

[15] T. Duckett, S. Marsland, and J. Shapiro, "Fast, on-line learning of globally consistent maps," *Autonomous Robots*, vol. 12, no. 3, pp. 287–300, 2002.

[16] E. Olson, J. Leonard, and S. Teller, "Fast iterative optimization of pose graphs with poor initial estimates," in *Proc. 2006 IEEE Int. Conf. on Robotics and Automation (ICRA)*, May 2006, pp. 2262–2269.

[17] G. Grisetti, C. Stachniss, S. Grzonka, and W. Burgard, "A tree parameterization for efficiently computing maximum likelihood maps using gradient descent," in *Robotics: Science and Systems III*, Atlanta, GA, USA, June 2007.

[18] S. Thrun and J. J. Leonard, "Simultaneous localization and mapping," in *Springer Handbook of Robotics*, B. Siciliano and O. Khatib, Eds. Springer Berlin/Heidelberg, 2008, pp. 871–889.

[19] M. Buettner and D. Wetherall, "An empirical study of UHF RFID performance," in *Proc. 14th ACM Int. Conf. on Mobile Computing and Networking (MobiCom)*, 2008, pp. 223–234.

[20] F. Savelli and B. Kuipers, "Loop-closing and planarity in topological map-building," in *Proc. IEEE/RSJ Int. Conf. on Intelligent Robots and Systems (IROS)*, vol. 2, 2004, pp. 1511–1517.